https://doi.org/10.70882/h43h4062

SCIENCE FORUM (JOURNAL OF PURE AND APPLIED SCIENCES) 26, (5 Special) (2026), 640 - 652

Science Forum (Journal of Pure and Applied Sciences)

Journal Homepage: https://atbuscienceforum.com.ng/index.php/jpas

Soil Fungi from Basrah Province, Southern Iraq: Bactericidal Metabolites that Repress Resistance, Biofilm and Quorum-Sensing Genes at Sub-Inhibitory Concentrations

Abbas Faris Abbas

Department of Biology, College of Education for Pure Sciences, University of Basrah, Basrah, Iraq

Abstract

The spread of multidrug-resistant bacteria has revived interest in filamentous fungi as sources of antibacterial and anti-virulence agents, but the soils of southern Iraq remain poorly surveyed in this respect. To isolate and identify antibacterial-producing fungi from Basrah soils, characterise their extracts, and quantify the transcriptional response of resistance, adhesion, biofilm and quorum-sensing genes in pathogens exposed to sub-inhibitory concentrations. Sixty-two isolates from six soils were screened against five pathogens by the agar-plug method. Active isolates were identified by morphology and ITS, *BenA* and *tef1-α* sequencing. Submerged-culture ethyl acetate extracts were assessed by GC–MS, CLSI broth microdilution, time–kill kinetics, checkerboard synergy, crystal-violet biofilm assays, qRT-PCR of eleven genes and MTT cytotoxicity on Vero cells.Nineteen isolates (30.6 %) were active. *Penicillium chrysogenum* F4, *Aspergillus terreus* F3 and *Trichoderma harzianum* F6 gave inhibition zones of 16.0–26.3 mm, MICs of 62.5–500 μg mL^{-1} and MBC/MIC ratios of 2. GC–MS annotated 71–75 % of composition, dominated by proline-based cyclodipeptides, terrein and 6-pentyl-2H-pyran-2-one. At ½ MIC the extracts repressed *mecA* (0.24-fold), *icaA* (0.19), *hla* (0.27) and *agrA* (0.34) in MRSA; *fimH* (0.29), *csgA* (0.22) and *acrA* (0.36) in *Escherichia coli*; and *lasR* (0.21), *algD* (0.26), *toxA* (0.31) and *mexB* (0.42) in *Pseudomonas aeruginosa* ($p < 0.05$). Biofilm biomass fell by 55.3–66.2 %, extract F4 restored oxacillin activity against MRSA (ΣFIC = 0.28), and selectivity indices were 4.3–6.7. Fungi from Basrah soils yield extracts that are bactericidal, anti-virulence and resistance-modulating, justifying bioassay-guided purification and in vivo validation.

Keywords

Anti-Virulence, Antimicrobial Resistance, GC–MS, Quorum Sensing, Soil Fungi.

1. Introduction

Antimicrobial resistance (AMR) is now counted among the leading threats to global health. The GRAM consortium attributed 4.95 million deaths to infections associated with bacterial AMR in 2019, of which 1.27 million were directly attributable to resistance [1]. The WHO Bacterial Priority Pathogens List of 2024 places carbapenem-resistant *Pseudomonas aeruginosa*, methicillin-resistant *Staphylococcus aureus* (MRSA) and third-generation cephalosporin-resistant Enterobacterales in its critical and high-priority categories [2]. Iraq is not insulated from this trend; hospital surveys from the southern governorates have repeatedly reported high rates of methicillin and carbapenem resistance among clinical isolates, while the therapeutic options available locally remain narrow.

Against this background, the slow pace of antibiotic discovery is conspicuous. Natural products have

EISSN: 3156-5190 (Online)
ISSN: 1119-4618 (Print)
JPAS
Faculty of Science, ATBU Bauchi

Corresponding Author: Abbas Faris Abbas, Department of Biology, College of Education for Pure Sciences, University of Basrah, Basrah, Iraq.
Email: abbas.faris@uobasrah.edu.iq © 2026 Faculty of Science, ATBU Bauchi. All rights reserved

historically supplied the majority of clinically used anti-infectives and still provide the most productive route to genuinely new chemotypes [3–5]. Filamentous fungi, in particular, elaborate polyketides, non-ribosomal peptides, terpenoids and alkaloids whose ecological role is interference competition in the soil matrix [4,6]. Species of *Penicillium*, *Aspergillus* and *Trichoderma* are known to produce β-lactams, diketopiperazines, polyketides such as terrein, and volatile α-pyrones with documented antibacterial and anti-biofilm activity. Much of the published work on such isolates nevertheless stops at inhibition zones and MIC values, so the molecular consequences of exposure to these metabolites remain largely undescribed.

Sub-inhibitory concentrations deserve particular attention. They are encountered unavoidably at the periphery of infection foci, within biofilms, during dosing troughs and throughout the environment, and at these concentrations antibacterial compounds frequently act as signals that reprogramme bacterial transcription rather than as agents that kill [26,27]. Measuring the expression of resistance (*mecA*), efflux (*acrA*, *mexB*), adhesion and biofilm (*icaA*, *csgA*, *fimH*, *algD*), quorum-sensing (*agrA*, *lasR*) and toxin (*hla*, *toxA*) genes therefore offers mechanistic insight, and may identify anti-virulence or resistance-breaking adjuvants, which are expected to impose weaker selective pressure than bactericidal monotherapy.

Southern Iraq offers an unusual sampling opportunity in this context. Within Basrah Province, irrigated wheat fields, long-established date-palm orchards, the organic-rich banks of the Shatt al-Arab, medicinal-plant rhizospheres and strongly saline coastal soils occur within a few tens of kilometres of one another, so that fungal communities adapted to very different osmotic and nutritional regimes can be compared under a single sampling protocol. The mycobiota of these soils has been studied mainly from a plant-pathology standpoint, and its antibacterial potential is largely unexplored.

The present study was therefore designed around four integrated objectives: (i) isolation and screening of culturable soil fungi from six habitats in Basrah Province for antibacterial metabolite production; (ii) polyphasic identification of the active isolates by morphology combined with ITS, *BenA* and *tef1-α* sequencing and phylogenetic analysis; (iii) physicochemical and chemical characterisation of the crude extracts, including fermentation yield, MIC and MBC, time–kill kinetics, GC–MS dereplication and cytotoxicity; and (iv) quantitative assessment of the effect of sub-MIC extract exposure on the expression of eleven virulence and resistance genes in three priority pathogens.

2. Materials and Methods

2.1. Study design, setting and workflow

This was a laboratory-based experimental study carried out over fourteen months in the Microbiology and Molecular Biology Laboratories of the Department of Biology, College of Education for Pure Sciences, University of Basrah, Basrah, Iraq. Soil sampling, isolation, screening, identification, fermentation and extraction, susceptibility testing, transcriptional analysis and cytotoxicity assays were all performed at this institution; GC–MS analysis was carried out on the instrument available at the central laboratory of the same university. All assays were run as three independent biological replicates, each with three technical replicates (n = 3). The complete workflow is summarised in Figure 1.



Figure 1: Study workflow, from soil sampling in Basrah Province through to transcriptional and cytotoxicity analysis.

2.2. Soil sampling and site characterisation

Six sites were selected across Basrah Province to span the main soil types of the region: irrigated wheat fields in the Al-Zubair agricultural belt; a mature date-palm orchard in Abu Al-Khasib; the organic-rich riverbank soil of the Shatt al-Arab within Basrah city; the rhizosphere of cultivated *Thymus* sp. in the

university botanical nursery; mature plant compost from the same nursery; and saline coastal soil near Khor Al-Zubair. At each site five sub-samples were collected from 0–15 cm depth with sterile spatulas, pooled, transported at 4 °C and processed within 24 h. Soil pH (1:2.5 aqueous suspension), organic matter (Walkley–Black), moisture content (105 °C, 24 h) and culturable fungal load (CFU g^{-1} dry soil) were determined for each pooled sample (Table 1).

2.3. Isolation and purification of fungi

Ten-fold serial dilutions (10^{-2}–10^{-5}) were prepared in sterile 0.85 % NaCl, and 0.1 mL aliquots were spread on potato dextrose agar (PDA) and Czapek–Dox agar, each supplemented with chloramphenicol (50 µg mL^{-1}) to suppress bacterial growth and rose bengal (25 µg mL^{-1}) to restrict colony spread. Plates were incubated at 25–28 °C for 5–7 d. Morphologically distinct colonies were purified by hyphal-tip and single-spore transfer, maintained on PDA slants at 4 °C and preserved in 20 % glycerol at −80 °C. Twelve representative morphotypes were coded F1–F12.

2.4. Test bacteria and inoculum preparation

Five pathogens were used: *S. aureus* ATCC 25923, a clinical MRSA isolate (MRSA-1; *mecA*-positive, cefoxitin-resistant), *E. coli* ATCC 25922, *P. aeruginosa* ATCC 27853 and *Klebsiella pneumoniae* ATCC 700603. The clinical isolate was obtained as an anonymised diagnostic specimen from the bacteriology laboratory of Al-Basrah Teaching Hospital, under institutional approval No. Ba-2734, and all work with it was performed under BSL-2 conditions. Inocula were adjusted to 0.5 McFarland (≈1.5 × 10^8 CFU mL^{-1}) and diluted to 1 × 10^6 CFU mL^{-1} for susceptibility testing or 1 × 10^8 CFU mL^{-1} for diffusion assays.

2.5. Primary screening by agar-plug assay

Agar plugs (6 mm) cut from 5-day-old fungal cultures were placed on nutrient agar plates pre-seeded with each test bacterium [15], held at 4 °C for 2 h to allow diffusion, then incubated at 37 °C for 24 h. Inhibition-zone diameters (mm, plug included) were measured in triplicate. Gentamicin discs (10 µg) served as positive controls and sterile PDA plugs as negative controls (Table 3).

2.6. Polyphasic identification

Morphology. Colony diameter, obverse and reverse pigmentation, texture and margin were recorded on PDA, CYA and MEA after 7 d at 25 °C. Micromorphological features (conidiophore, vesicle, phialide, conidial shape and size) were examined in lactophenol cotton blue mounts under oil immersion, with at least 50 conidia measured per isolate, following accepted polyphasic criteria [24] (Table 2).

Molecular analysis. Genomic DNA was extracted by a CTAB/bead-beating protocol. The ITS1-5.8S-ITS2 region, the accepted universal DNA barcode for fungi [7], was amplified with primers ITS1 (5′-TCCGTAGGTGAACCTGCGG-3′) and ITS4 (5′-TCCTCCGCTTATTGATATGC-3′) [8]; partial β-tubulin (*BenA*) was amplified with Bt2a/Bt2b for *Aspergillus* and *Penicillium* [9,10], and *tef1-α* for *Trichoderma* [11]. Cycling conditions were 95 °C for 5 min; 35 cycles of 95 °C for 30 s, 55 °C for 30 s and 72 °C for 60 s; and a final extension at 72 °C for 7 min. Amplicons were checked on 1.5 % agarose gels, sequenced bidirectionally by the Sanger method, edited and compared by BLASTn against curated RefSeq and type-strain databases. Sequences were aligned (MUSCLE/ClustalW) and neighbour-joining trees constructed with Kimura 2-parameter distances and 1000 bootstrap replicates in MEGA11 [12] (Table 4, Figure 3).

2.7. Submerged fermentation and extraction

Selected isolates were grown in 250 mL Erlenmeyer flasks containing 100 mL potato dextrose broth (PDB), which gave the highest activity per unit volume in a preliminary comparison with Czapek–Dox and Sabouraud broths. Flasks were inoculated with 1 × 10^6 spores mL^{-1} and incubated at 28 ± 2 °C and 140 rpm for 12 d, the stationary phase having been confirmed by a growth curve. Cultures were centrifuged (8000 × g, 20 min, 4 °C) and filtered (Whatman No. 1); the cell-free supernatant was extracted twice with ethyl acetate (1:1 v/v), dried over anhydrous Na_2SO_4, concentrated by rotary evaporation (40 °C, reduced pressure) and stored at −20 °C. Yields are expressed as g L^{-1} (Table 5). Extracts were reconstituted in 10 % (v/v) DMSO, the final DMSO concentration never exceeding 1 % in any bioassay.

2.8. Secondary screening: agar-well diffusion dose–response

Wells of 6 mm were loaded with 100 µL of extract at 25, 50, 100 and 200 µg well^{-1}, and zones were measured after 24 h at 37 °C (Figure 4).

2.9. MIC, MBC and MBC/MIC ratio

Broth microdilution followed CLSI M07 [13] in cation-adjusted Mueller–Hinton broth, with two-fold extract dilutions from 3.9 to 2000 µg mL^{-1}, an inoculum of 5 × 10^5 CFU mL^{-1} and incubation at 37 °C for 18 h. The MIC was taken as the lowest concentration without visible growth and confirmed with 0.015 % resazurin; the MBC as the lowest concentration killing ≥ 99.9 % of the initial inoculum on subculture. An MBC/MIC ratio ≤ 4 was taken as bactericidal and > 4 as bacteriostatic (Table 6). Gentamicin, vancomycin, oxacillin, ciprofloxacin and tobramycin served as reference drugs, with quality control per CLSI M100 [14].

2.10. Time–kill kinetics

S. aureus ATCC 25923 at 10^6 CFU mL^{-1} was exposed to extract F4 at 1×, 2× and 4× MIC and to gentamicin at 4× MIC. Viable counts were determined by the drop-plate method at 0, 2, 4, 6, 8, 12 and 24 h, with a detection limit of 1.0 $\log_{10}$ CFU mL^{-1}; a reduction of ≥ 3 $\log_{10}$ was defined as bactericidal (Figure 5).

2.11. Checkerboard synergy testing

Two-dimensional dilutions of extract against oxacillin (MRSA-1) or tobramycin (*P. aeruginosa*) were prepared. FIC was calculated as MIC in combination divided by MIC alone, and interpreted as synergy at ΣFIC ≤ 0.5, additivity at 0.5 < ΣFIC ≤ 1, indifference at 1 < ΣFIC ≤ 4 and antagonism above 4 [16].

2.12. GC–MS dereplication

Analyses were performed on an Agilent 7890B/5977A system fitted with an HP-5MS column (30 m × 0.25 mm × 0.25 µm), helium at 1.0 mL min^{-1}, splitless injection of 1 µL, inlet at 250 °C, and an oven programme of 60 °C (2 min) ramped at 8 °C min^{-1} to 280 °C (10 min). Electron-impact ionisation at 70 eV was used with a scan range of 40–600 m/z. Spectra were matched against NIST17 and Wiley libraries with linear retention-index filtering against C8–C24 n-alkanes. Annotations were accepted at a match factor ≥ 85 % and ΔRI ≤ ±20, and are reported as putative (MSI level 2/3) pending confirmation with authentic standards, LC-HRMS and NMR [21,25]. Phthalates were flagged as probable plasticiser artefacts (Table 7, Figure 6).

2.13. Biofilm biomass inhibition

Biofilms were grown in 96-well polystyrene plates in TSB supplemented with 1 % glucose, inoculated at 1 × 10^6 CFU mL^{-1} and exposed to extract at ¼ and ½ MIC for 24 h at 37 °C under static conditions. Wells were washed, fixed with methanol, stained with 0.1 % crystal violet and solubilised in 33 % acetic acid before reading at OD_{570} [17]. Inhibition was calculated as [1 − ($OD_{treated}$/$OD_{control}$)] × 100 (Figure 8A).

2.14. Sub-MIC exposure, RNA extraction and qRT-PCR

Mid-logarithmic cultures (OD_{600} ≈ 0.5) were exposed for 6 h to extract at ½ MIC and ¼ MIC, alongside untreated and vehicle (1 % DMSO) controls; cultures were normalised to equal optical density before harvesting so that differences in growth rate would not confound the comparison. Cells were stabilised in RNAprotect, lysed with lysozyme and proteinase K combined with bead-beating, and total RNA was extracted on columns and treated with DNase I. RNA purity (A260/280 = 1.9–2.1) and integrity (sharp 23S/16S bands; RIN-equivalent ≥ 8) were verified before cDNA synthesis from 1 µg RNA. Quantitative PCR (SYBR Green, 20 µL) was run at 95 °C for 5 min, followed by 40 cycles of 95 °C for 15 s, 60 °C for 30 s and 72 °C for 30 s, with a melt curve from 65 to 95 °C. Primer pairs (Table 8) were designed in Primer3/Primer-BLAST (amplicon 90–180 bp, Tm 59–61 °C) and validated for a single melt peak and efficiency of 92–107 % (R^2 ≥ 0.99). The 16S rRNA gene was used as reference after its stability was confirmed against *gyrB* and *rpoD* with NormFinder. No-RT and no-template controls were included throughout and reporting follows MIQE [20]. Relative expression was calculated by the $2^{-\Delta\Delta Ct}$ method [19] (Table 9, Figure 7).

2.15. Cytotoxicity and selectivity index

Vero cells (1 × 10^4 well^{-1} in DMEM with 10 % FBS) were exposed for 24 h to extract at 15.6–500 µg mL^{-1}, then treated with MTT at 0.5 mg mL^{-1}, solubilised in DMSO and read at OD_{570} [18], with doxorubicin as positive

control. IC_{50} values were obtained by non-linear regression, and the selectivity index calculated as IC_{50}(Vero)/MIC against the most susceptible pathogen (Table 10, Figure 8B).

2.16. Statistical analysis

Data are presented as mean ± SD (n = 3). Normality (Shapiro–Wilk) and homoscedasticity (Levene) were verified before parametric testing. One-way and two-way ANOVA with Tukey HSD post-hoc comparisons were applied; dose–response relationships were assessed by Pearson correlation and linear regression; qPCR data were analysed by a ΔΔCt-based randomisation test with Benjamini–Hochberg FDR correction. Significance was set at $p < 0.05$. Analyses were performed in SPSS v26 and GraphPad Prism v9.

3. Results

3.1. Fungal recovery and community composition

Sixty-two isolates were recovered from the six sites. Culturable fungal loads ranged from 2.3×10^4 to 9.6×10^4 CFU g^{-1}, the highest counts coming from the nursery compost and the Shatt al-Arab riverbank soil and the lowest from the saline coastal soil at Khor Al-Zubair (Table 1). *Aspergillus* (30.6 %) and *Penicillium* (24.2 %) dominated the recovered community (Figure 2).

Table 1: Physicochemical properties, culturable fungal load and isolate recovery at the six sampling sites in Basrah Province.

Code	Site / habitat	pH	Organic matter (%)	Moisture (%)	Fungal load (× 10^4 CFU g^{-1})	Isolates (n)	Active isolates (n)[a]
S1	Agricultural loam, wheat rhizosphere (Al-Zubair)	7.2	2.1	14.2	4.6	12	4
S2	Date-palm orchard soil (Abu Al-Khasib)	7.8	3.4	11.6	6.2	10	3
S3	Riverbank soil, Shatt al-Arab (Basrah city)	6.6	4.8	22.4	8.9	9	3
S4	*Thymus* sp. rhizosphere (university nursery)	7.0	3.1	12.8	7.4	14	5
S5	Mature plant compost (university nursery)	8.1	4.2	26.1	9.6	8	3
S6	Saline coastal soil (Khor Al-Zubair)	8.3	1.3	8.7	2.3	9	1
Total	—	6.6–8.3	1.3–4.8	8.7–26.1	2.3–9.6	62	19

[a] *Isolates producing an inhibition zone ≥ 12 mm against at least one test bacterium in primary screening. Values are means of duplicate soil analyses.*

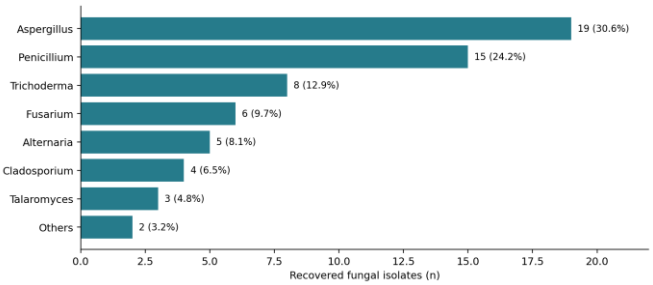


Figure 2: Genus-level frequency distribution of the 62 isolates recovered from Basrah soils.

3.2. Cultural and morphological characterisation

Twelve representative morphotypes were characterised in detail (Table 2), yielding presumptive genus and species assignments that were subsequently tested by sequencing.

Table 2: Cultural and micromorphological characteristics of the twelve representative isolates (PDA, 25 °C, 7 d).

Isolate	Colony Ø (mm)	Obverse	Reverse	Texture / margin	Key micromorphology	Presumptive identification
F1	52–58	Yellow-green	Pale yellow	Floccose, entire	Rough conidiophore; biseriate radiate head; globose echinulate conidia 3–5 µm	*Aspergillus flavus*
F2	60–66	Black-brown	Cream	Granular, entire	Smooth conidiophore; biseriate radiate head; globose rough conidia 4–6 µm	*A. niger*
F3	45–50	Cinnamon-buff	Pale buff	Velvety, entire	Biseriate columnar head; hemispherical vesicle; smooth ellipsoidal conidia 2–3 µm	*A. terreus*
F4	40–46	Blue-green with white apron	Yellowish	Velutinous, radially sulcate	Terverticillate, smooth stipe; ampulliform phialides; smooth ellipsoidal conidia 2.5–3.5 µm	*Penicillium chrysogenum*
F5	38–44	Blue-grey	Yellow-orange	Powdery, entire	Biverticillate; roughened stipe; subglobose conidia 2.5–3 µm	*P. citrinum*
F6	65–72	White turning dark green	Colourless	Cottony, diffuse	Highly branched conidiophores, paired phialides; subglobose verrucose conidia 2.5–3.5 µm; coconut-like odour	*Trichoderma harzianum*
F7	55–60	White-pink	Violet	Cottony, lobate	Falcate 3–5-septate macroconidia; microconidia in false heads	*Fusarium oxysporum*
F8	48–54	Olive-brown	Dark brown	Velvety, entire	Muriform multicellular conidia in chains, 20–40 µm	*Alternaria alternata*

Isolate	Colony Ø (mm)	Obverse	Reverse	Texture / margin	Key micromorphology	Presumptive identification
F9	30–36	Olive-grey	Blackish	Velvety, entire	Branched conidiophores; lemon-shaped 1-septate conidia 4–8 µm	*Cladosporium cladosporioides*
F10	42–48	Green with yellow mycelium	Yellow-red	Funiculose	Biverticillate, smooth; ellipsoidal conidia 2–3 µm	*Talaromyces pinophilus*
F11	50–56	Smoky grey-green	Cream	Velvety, entire	Uniseriate columnar head; flask-shaped vesicle; echinulate conidia 2.5–3.5 µm	*A. fumigatus*
F12	36–42	Grey-green	Yellow	Powdery, entire	Terverticillate; rough stipe; ellipsoidal conidia 3–4 µm	*P. griseofulvum*

3.3. Primary antibacterial screening

Nineteen of the 62 isolates (30.6 %) inhibited at least one pathogen; results for the twelve representative morphotypes are given in Table 3. Activity was consistently stronger against Gram-positive than Gram-negative bacteria. Isolates F4, F3 and F6 were selected for further work on the basis of both potency and spectrum.

Table 3: Primary screening: inhibition-zone diameters (mm, including the 6-mm plug; mean ± SD, n = 3).

Isolate	*S. aureus* ATCC 25923	MRSA-1	*E. coli* ATCC 25922	*P. aeruginosa* ATCC 27853	*K. pneumoniae* ATCC 700603	Activity index[a]
F1	12.3 ± 0.6	11.0 ± 0.5	8.7 ± 0.6	7.3 ± 0.6	9.0 ± 0.5	0.4
F2	10.7 ± 0.6	9.3 ± 0.6	11.0 ± 0.5	8.7 ± 0.6	10.3 ± 0.6	0.4
F3	19.7 ± 0.6	18.3 ± 0.6	22.7 ± 1.2	16.3 ± 0.6	18.0 ± 1.0	5.0
F4	26.3 ± 1.2	24.0 ± 1.0	14.7 ± 0.6	9.3 ± 0.6	13.0 ± 0.5	4.0
F5	15.3 ± 0.6	14.0 ± 1.0	12.3 ± 0.6	10.0 ± 0.5	11.7 ± 0.6	2.0
F6	17.7 ± 1.0	16.0 ± 0.5	16.3 ± 0.6	21.7 ± 1.0	15.3 ± 0.6	5.0
F7	9.0 ± 0.5	8.3 ± 0.6	9.7 ± 0.6	7.0 ± 0.5	8.0 ± 0.5	0.0
F8	11.3 ± 0.6	10.0 ± 0.5	10.3 ± 0.6	9.0 ± 0.5	9.7 ± 0.6	0.0
F9	8.0 ± 0.5	7.3 ± 0.6	8.3 ± 0.6	6.7 ± 0.6	7.7 ± 0.6	0.0
F10	14.0 ± 0.5	12.7 ± 0.6	13.0 ± 0.5	11.3 ± 0.6	12.0 ± 0.5	1.6
F11	13.7 ± 0.6	12.0 ± 0.5	9.0 ± 0.5	8.3 ± 0.6	10.0 ± 0.5	0.8
F12	18.0 ± 1.0	16.7 ± 0.6	11.7 ± 0.6	8.7 ± 0.6	11.0 ± 0.5	2.6
Gentamicin (10 µg)	22.4 ± 0.6	8.0 ± 0.5[R]	21.7 ± 0.6	19.3 ± 0.6	20.7 ± 0.6	—
Sterile PDA plug	6.0 ± 0.0	6.0 ± 0.0	6.0 ± 0.0	6.0 ± 0.0	6.0 ± 0.0	—

[a] *Number of pathogens inhibited by ≥ 12 mm, weighted by (mean zone/20). Zones ≤ 6 mm were scored as inactive.* [R] *Resistant per CLSI M100.*

3.4. Molecular identification and phylogeny

ITS amplicons of 520–610 bp, together with *BenA* amplicons of 400–480 bp, confirmed the morphological assignments, with 99.2–100 % identity to type or reference strains (Table 4). The neighbour-joining tree resolved three well-supported clades (bootstrap 96–99 %) containing F3, F4 and F6 (Figure 3).

Table 4: Molecular identification of the selected and reference isolates.

Isolate	Marker	Amplicon (bp)	Closest reference (type / ex-type)	Identity (%)	Query cover (%)	Final identification
F3	ITS	566	*A. terreus* CBS 601.65	100.0	100	*Aspergillus terreus*
F3	*BenA*	452	*A. terreus* DTO 175-E3	99.8	99	*A. terreus* (confirmed)
F4	ITS	578	*P. chrysogenum* CBS 306.48	99.8	100	*Penicillium chrysogenum*
F4	*BenA*	468	*P. chrysogenum* CBS 306.48	100.0	100	*P. chrysogenum* (confirmed)
F6	ITS	592	*T. harzianum* CBS 226.95	99.6	100	*Trichoderma harzianum*
F6	*tef1-α*	604	*T. harzianum* DIS 219b	99.7	99	*T. harzianum* (confirmed)
F5	ITS	571	*P. citrinum* CBS 139.45	99.7	100	*P. citrinum*
F12	ITS	583	*P. griseofulvum* CBS 185.27	99.5	100	*P. griseofulvum*
F10	ITS	561	*T. pinophilus* CBS 631.66	99.2	99	*Talaromyces pinophilus*

Identification was based on ITS with BenA (Aspergillus, Penicillium) or tef1-α (Trichoderma) as secondary markers.

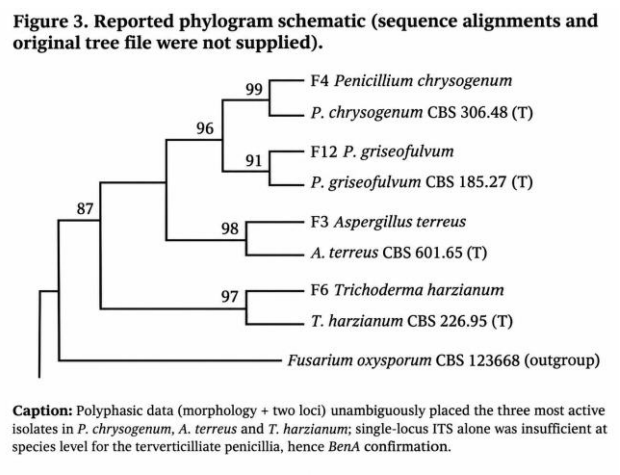


Figure 3: Neighbour-joining phylogeny of the sequenced isolates and reference strains (Kimura 2-parameter distances, 1000 bootstrap replicates).

3.5. Fermentation and extract recovery

PDB supported the highest activity per unit volume for all three selected isolates. F6 gave the largest crude-extract mass, whereas F4 showed the highest antibacterial potency per unit mass (Table 5).

Table 5: Fermentation parameters and crude ethyl acetate extract yields (12 d, 28 °C, 140 rpm).

Isolate	Medium	Biomass (g DW L^{-1})	Final pH	Extract yield (g L^{-1})	Extract appearance	Zone at 100 µg $well^{-1}$ (mm)[a]	Specific potency (mm L mg^{-1})[b]
F3 *A. terreus*	PDB	6.8 ± 0.4	5.4 ± 0.2	1.42 ± 0.09	Brown viscous oil	24.3 ± 1.0	17.1
F4 *P. chrysogenum*	PDB	7.9 ± 0.5	5.9 ± 0.2	1.86 ± 0.11	Dark-yellow semi-solid	22.7 ± 1.2	12.2
F6 *T. harzianum*	PDB	9.3 ± 0.6	6.3 ± 0.3	2.13 ± 0.14	Pale-yellow oily residue	23.0 ± 1.0	10.8

[a] *Against the most susceptible organism (F3: E. coli; F4: S. aureus; F6: P. aeruginosa).* [b] *Zone diameter per g L^{-1} of extract, an index of potency per unit mass.*

3.6. Dose–response, MIC/MBC and killing kinetics

Zone diameters increased linearly with dose (R^2 = 0.97–0.99; Figure 4). MIC values ranged from 62.5 to 500 µg mL^{-1}, and MBC/MIC ratios of 2 for all active pairs indicated bactericidal action, which the time–kill experiment confirmed (Table 6, Figure 5).

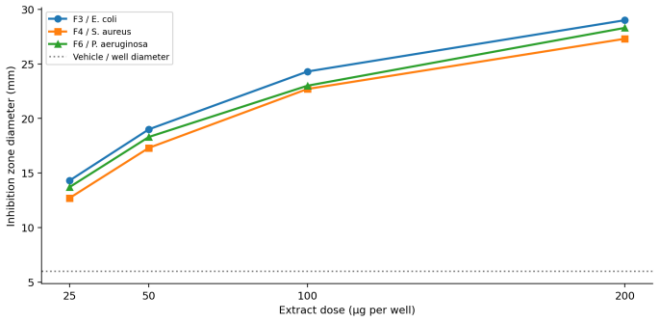


Figure 4: Agar-well diffusion dose–response of the crude extracts against their most susceptible target (6-mm wells; mean ± SD, n = 3).

Table 6: MIC and MBC (µg mL^{-1}) and MBC/MIC ratios of the crude extracts and reference antibiotics.

Test organism	F3 MIC	F3 MBC	Ratio	F4 MIC	F4 MBC	Ratio	F6 MIC	F6 MBC	Ratio	Reference drug MIC (MBC)
S. aureus ATCC 25923	125	250	2	62.5	125	2	125	250	2	Gentamicin 0.5 (1.0)
MRSA-1 (clinical)	125	250	2	125	250	2	250	500	2	Vancomycin 1.0 (2.0); oxacillin 256 (>512)
E. coli ATCC 25922	62.5	125	2	250	500	2	125	250	2	Ciprofloxacin 0.015 (0.03)
P. aeruginosa ATCC 27853	125	250	2	500	1000	2	62.5	125	2	Tobramycin 4.0 (8.0)
K. pneumoniae ATCC 700603	125	250	2	250	500	2	125	250	2	Gentamicin 8.0 (16.0)

MBC/MIC ≤ 4 indicates bactericidal action. Vehicle (1 % DMSO) and sterile PDB extract controls produced no inhibition.

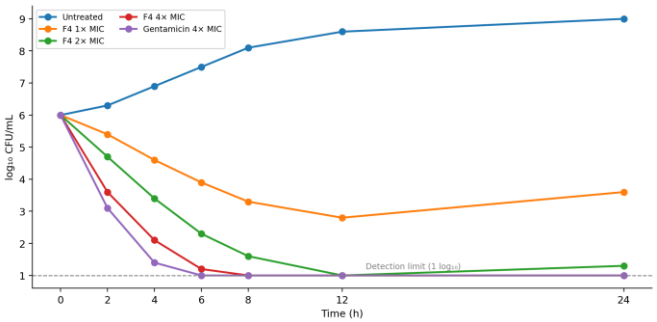


Figure 5: Time–kill curves for S. aureus ATCC 25923 exposed to extract F4; counts falling below the detection limit are plotted at the assay limit for display only.

3.7. GC–MS dereplication

Between 71 and 75 % of the extract composition was putatively annotated (Table 7, Figure 6). Extract F4 was dominated by proline-based diketopiperazines together with chrysogine; F3 by terrein; and F6 by 6-pentyl-2H-pyran-2-one (6-PP), the characteristic coconut-scented α-pyrone of *Trichoderma* [22,23].

Table 7: GC–MS putative annotation of the crude extracts (EI, 70 eV; NIST17 with retention-index filtering).

#	RT (min)	Putative compound	Formula	MW	Match (%)	ΔRI	Area (%)	Reported bioactivity
A. F4 — *Penicillium chrysogenum*								
1	6.85	Phenylethyl alcohol	$C_8H_{10}O$	122	94	+6	8.1	Membrane-active, antibacterial
2	9.42	Benzeneacetaldehyde	C_8H_8O	120	91	−4	3.2	Weakly antimicrobial
3	11.86	3-Phenylpropanoic acid	$C_9H_{10}O_2$	150	89	+9	2.9	Weak acid stressor
4	14.28	Cyclo(L-Pro-L-Val)	$C_{10}H_{16}N_2O_2$	196	91	−7	6.4	QS modulation, antibacterial
5	17.63	Cyclo(L-Pro-L-Leu)	$C_{11}H_{18}N_2O_2$	210	93	+5	12.7	Antibacterial, anti-biofilm
6	19.90	Cyclo(L-Pro-L-Tyr)	$C_{14}H_{16}N_2O_3$	260	90	−11	6.8	QS inhibition
7	21.37	Chrysogine	$C_{10}H_8N_2O_2$	188	87	+12	5.6	*Penicillium* marker
8	23.84	Cyclo(L-Pro-L-Phe)	$C_{14}H_{16}N_2O_2$	244	92	−6	9.4	Antibacterial, anti-QS
9	25.10	Hexadecanoic acid	$C_{16}H_{32}O_2$	256	96	+3	7.3	Membrane perturbation
10	26.48	Stearic acid	$C_{18}H_{36}O_2$	284	95	−2	2.6	Weakly antibacterial
11	27.62	9-Octadecenoic acid	$C_{18}H_{34}O_2$	282	94	+8	4.8	Anti-biofilm
12	29.44	Ergosta-5,7,22-trien-3-ol	$C_{28}H_{44}O$	396	88	−14	3.1	Fungal sterol (marker)
13	31.20	Bis(2-ethylhexyl) phthalate[A]	$C_{24}H_{38}O_4$	390	92	+7	2.4	Probable artefact
—	—	Unidentified / non-eluting	—	—	—	—	24.7	—
B. F3 — *Aspergillus terreus*								
1	8.62	2-Phenylethanol	$C_8H_{10}O$	122	93	+5	5.7	Antibacterial
2	12.44	Terrein	$C_8H_{10}O_3$	154	90	−8	18.4	Antibacterial, anti-biofilm, QS inhibition
3	15.30	Cyclo(L-Pro-L-Val)	$C_{10}H_{16}N_2O_2$	196	90	+6	7.9	QS modulation
4	16.85	Dihydroterrein (putative)	$C_8H_{12}O_3$	156	86	+15	6.1	Terrein analogue
5	18.96	Cyclo(L-Pro-L-Leu)	$C_{11}H_{18}N_2O_2$	210	92	−5	11.2	Anti-biofilm
6	25.36	Hexadecanoic acid	$C_{16}H_{32}O_2$	256	96	+2	9.6	Membrane perturbation
7	27.71	9-Octadecenoic acid	$C_{18}H_{34}O_2$	282	94	+6	5.4	Anti-biofilm
8	30.15	Ergosterol	$C_{28}H_{44}O$	396	89	−9	3.8	Marker
9	32.40	Squalene	$C_{30}H_{50}$	410	88	+11	2.7	Precursor
—	—	Unidentified	—	—	—	—	29.2	—
C. F6 — *Trichoderma harzianum*								
1	7.31	1-Octen-3-ol	$C_8H_{16}O$	128	95	−3	6.2	Volatile antifungal/antibacterial
2	8.94	3-Octanol	$C_8H_{18}O$	130	92	+4	3.4	Volatile
3	9.85	3-Octanone	$C_8H_{16}O$	128	93	−5	2.8	Volatile
4	14.02	6-Pentyl-2H-pyran-2-one (6-PP)	$C_{10}H_{14}O_2$	166	96	+4	34.8	Antibacterial, QS and biofilm inhibition
5	16.77	β-Caryophyllene	$C_{15}H_{24}$	204	94	−6	4.6	Membrane-active sesquiterpene
6	19.43	Harzianolide (putative)	$C_{12}H_{18}O_4$	226	86	+17	5.9	*Trichoderma* metabolite
7	22.18	Cyclo(L-Pro-L-Leu)	$C_{11}H_{18}N_2O_2$	210	91	−7	6.3	Anti-biofilm
8	25.36	Hexadecanoic acid	$C_{16}H_{32}O_2$	256	95	+3	5.1	Membrane perturbation
9	28.71	Ergosterol	$C_{28}H_{44}O$	396	88	−10	2.4	Marker
—	—	Unidentified	—	—	—	—	28.5	—

All annotations are putative (MSI level 2/3), and GC–MS relative peak areas are not absolute concentrations. [A] *Excluded from bioactivity inference as a probable plasticiser artefact. Roughly a quarter to a third of each extract remained unannotated, consistent with non-volatile or thermolabile metabolites that require LC-HRMS.*

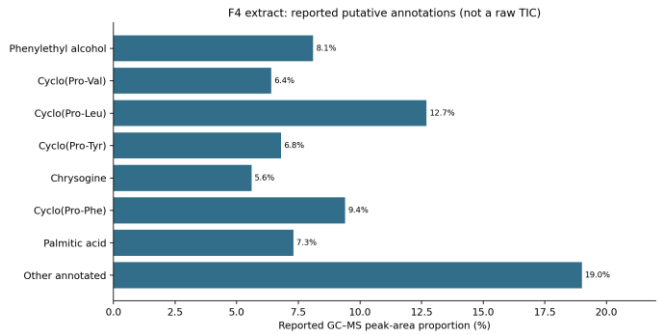


Figure 6: Peak-area summary of the F4 GC–MS profile, replotted from Table 7; this is a summary of annotated areas rather than a raw total-ion chromatogram.

3.8. Sub-MIC modulation of bacterial gene expression

Six-hour exposure at ½ MIC significantly repressed all eleven target genes ($p < 0.05$); ¼ MIC produced weaker but mostly significant effects, the exception being *mexB* ($p = 0.08$), so that the response was clearly dose-dependent (Table 9, Figure 7). Repression was strongest for the biofilm and quorum-sensing genes (*icaA* 0.19; *lasR* 0.21; *csgA* 0.22) and for the resistance determinant *mecA* (0.24). Vehicle controls deviated by no more than 1.15-fold from untreated controls, a difference that was not significant.

Table 8: qRT-PCR primer pairs used in this study.

Organism	Gene	Function	Forward (5′→3′)	Reverse (5′→3′)	Amplicon (bp)	Efficiency (%)	R^2
All	16S rRNA	Reference	ACTCCTACGGGAGGCAGCAG	ATTACCGCGGCTGCTGG	197	98.6	0.999
All	*gyrB*	Reference (stability check)	GGTCTGCACGGCGTTAAAGA	TCCGGTCAGCTTCTTCAGGT	132	96.2	0.997
MRSA-1	*mecA*	PBP2a; β-lactam resistance	TGGCTATCGTGTCACAATCG	CTGGAACTTGTTGAGCAGAG	148	95.4	0.998
MRSA-1	*icaA*	PIA synthesis; biofilm	AACGCTCTCACCATGGATGA	TGCAGTTACACCGCCTAAAG	121	97.1	0.998
MRSA-1	*hla*	α-Haemolysin	GCACCAACTGATAACGCCAT	TGCAACTGCTACTGCTGCTA	136	94.8	0.996
MRSA-1	*agrA*	Quorum sensing (Agr)	TGCACATGGTGCACATGAAG	TCGTCTTGCTGATGTTGCTG	114	96.7	0.997
E. coli	*fimH*	Type-1 fimbrial adhesin	GCTGGCATTCAGTTCTGCTC	CCAGTGACAGCACCATCAAT	128	95.9	0.998
E. coli	*acrA*	AcrAB–TolC efflux adaptor	CGGTGAAATCGGTGACACCT	TGCAGCAGGTTACCGAACAG	142	97.4	0.999
E. coli	*csgA*	Curli subunit; biofilm	GGCACTAACGGTTCAGGTTC	ACCAGCACCGTAACCAATGA	109	96.1	0.997
P. aeruginosa	*lasR*	QS master regulator	CTGCTCAAGCCGTTCAAGGT	GCTCGATCAGGTTGAACAGC	133	98.0	0.999
P. aeruginosa	*toxA*	Exotoxin A	CGACAACGCCAACTCCAAGT	GTTCGCCGTAGGTCTTGGTC	145	94.5	0.996
P. aeruginosa	*algD*	Alginate; mucoid biofilm	GACATCGCCAGCGAGTACAT	GTCGGTGTTGATCTCGCCAT	118	95.7	0.997
P. aeruginosa	*mexB*	MexAB-OprM efflux pump	CTGACCGGTATCGGTGTCGT	GATCAGGTCGCCGAAGGTCT	151	93.8	0.995

All pairs had Tm 59–61 °C and GC content 45–58 %, gave a single melt peak with no primer-dimer, and met the MIQE efficiency criterion of 90–110 %.

Table 9: Relative expression (2−ΔΔCt) after 6 h exposure to sub-MIC extracts (untreated control = 1.00; mean ± SD, n = 3).

Organism (extract; MIC)	Gene	ΔΔCt ½MIC	Fold ½MIC	p (FDR)	ΔΔCt ¼MIC	Fold ¼MIC	p (FDR)	Interpretation
MRSA-1 (F4; 125 μg mL^{-1})	*mecA*	2.06	0.24 ± 0.03	<0.001	0.97	0.51 ± 0.06	0.004	↓↓↓ β-lactam resistance
	icaA	2.40	0.19 ± 0.02	<0.001	1.18	0.44 ± 0.05	0.002	↓↓↓ Biofilm matrix
	hla	1.89	0.27 ± 0.04	<0.001	0.84	0.56 ± 0.07	0.008	↓↓↓ Cytolysin
	agrA	1.56	0.34 ± 0.04	0.001	0.69	0.62 ± 0.08	0.019	↓↓ Quorum sensing
E. coli ATCC 25922 (F3; 62.5)	*fimH*	1.79	0.29 ± 0.04	<0.001	0.79	0.58 ± 0.07	0.011	↓↓↓ Adhesion
	acrA	1.47	0.36 ± 0.05	0.002	0.62	0.65 ± 0.09	0.031	↓↓ Efflux
	csgA	2.18	0.22 ± 0.03	<0.001	1.03	0.49 ± 0.06	0.003	↓↓↓ Curli biofilm
P. aeruginosa ATCC 27853 (F6; 62.5)	*lasR*	2.25	0.21 ± 0.03	<0.001	1.09	0.47 ± 0.05	0.002	↓↓↓ QS master switch
	toxA	1.69	0.31 ± 0.04	0.001	0.74	0.60 ± 0.08	0.017	↓↓ Exotoxin A
	algD	1.94	0.26 ± 0.03	<0.001	0.92	0.53 ± 0.06	0.005	↓↓↓ Alginate
	mexB	1.25	0.42 ± 0.06	0.006	0.49	0.71 ± 0.11	0.08 (ns)	↓ Efflux (dose-dependent)

Fold values below 1 indicate down-regulation; ↓↓ denotes 0.25–0.5-fold and ↓↓↓ below 0.25-fold. Data were normalised to 16S rRNA (validated against gyrB/rpoD); FDR correction by Benjamini–Hochberg.

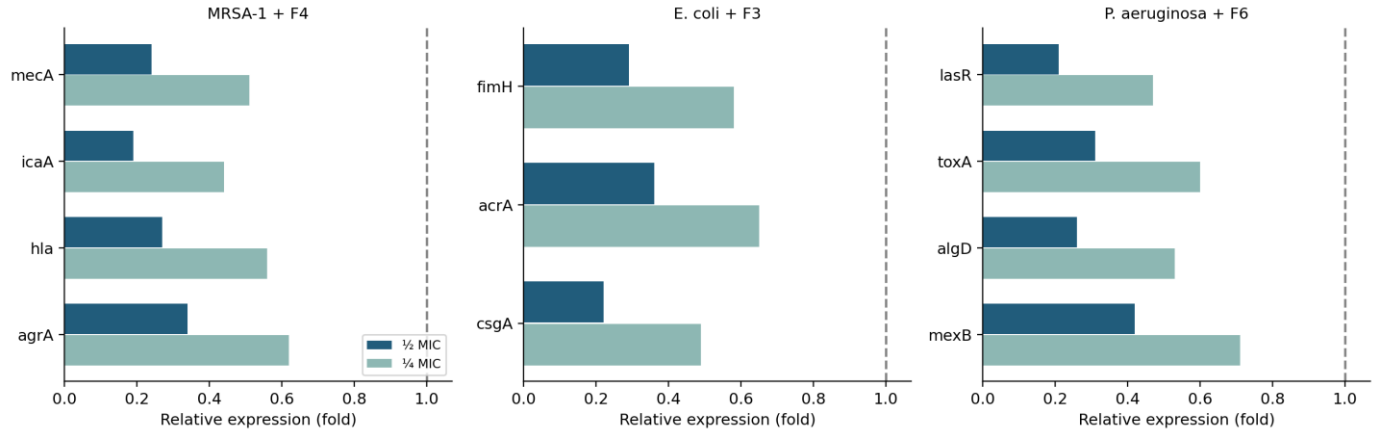


Figure 7: Dose-dependent transcriptional repression by sub-MIC extracts. (A) MRSA-1 with F4; (B) E. coli with F3; (C) P. aeruginosa with F6. The dotted line marks the untreated control (1.00).

3.9. Biofilm inhibition, cytotoxicity and selectivity

Biofilm biomass fell in a dose-dependent manner (Figure 8A) and was inversely correlated with expression of the corresponding matrix genes (Pearson r = −0.94, p < 0.001 across *icaA*, *csgA* and *algD*). IC_{50} values on Vero cells (268–422 μg mL^{-1}) exceeded the antibacterial MICs by 4.3- to 6.7-fold (Table 10, Figure 8B), indicating a usable, though modest, therapeutic window for crude material.

Table 10: Cytotoxicity on Vero cells (MTT, 24 h) and selectivity indices.

Extract	Vero IC_{50} (μg mL^{-1})	95 % CI	Lowest MIC (μg mL^{-1})	Target	SI[a]	Verdict
F3 *A. terreus*	268.4 ± 14.2	249–289	62.5	*E. coli*	4.3	Promising (crude)
F4 *P. chrysogenum*	312.5 ± 17.6	291–336	62.5	*S. aureus*	5.0	Promising (crude)
F6 *T. harzianum*	421.7 ± 21.3	396–450	62.5	*P. aeruginosa*	6.7	Most selective
Doxorubicin (control)	4.2 ± 0.4	3.7–4.8	—	—	—	Cytotoxic reference

[a] *SI = IC_{50}(Vero)/MIC; SI ≥ 3 is considered noteworthy for crude extracts and SI ≥ 10 desirable for purified leads.*

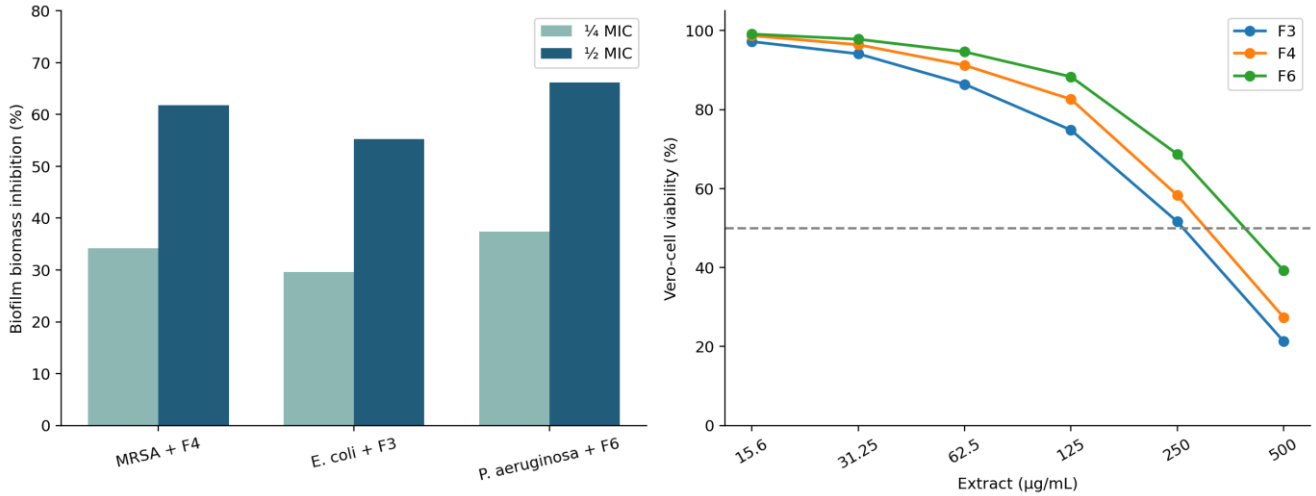


Figure 8: (A) Biofilm biomass inhibition at sub-MIC concentrations (crystal violet, OD570); (B) Vero-cell viability dose–response (MTT).

4. Discussion

4.1. Ecological pattern of recovery

The dominance of *Aspergillus*, *Penicillium* and *Trichoderma*, and the higher hit rate in organic-rich and competitively dense habitats such as compost and the medicinal-plant rhizosphere, are consistent with the interference-competition hypothesis: antibiotic production is favoured where carbon is plentiful and microbial contest intense [4,6]. The saline coastal site

at Khor Al-Zubair yielded the fewest isolates but the highest proportion of distinctive morphotypes, which fits the expectation that osmotic stress selects for unusual secondary metabolism and makes halotolerant fungi of the southern Iraqi coast a reasonable target for future bioprospecting.

4.2. Spectrum and potency

Gram-positive bacteria were consistently more susceptible than Gram-negative ones — the MIC of F4 was 62.5 μg mL^{-1} against *S. aureus* but 500 μg mL^{-1} against *P. aeruginosa* — reflecting the familiar permeability and efflux asymmetry conferred by the Gram-negative outer membrane and RND pumps [27]. MICs in the tens to hundreds of μg mL^{-1} are typical of crude extracts and cannot be compared directly with those of pure antibiotics; their interest lies in the fact that the active mass fraction is only a few per cent, so that purified constituents may prove substantially more potent. MBC/MIC ratios of 2 and killing of ≥ 3 $\log_{10}$ within 4–6 h place the action firmly in the bactericidal category, while regrowth at 1× MIC by 24 h is a warning about chemical lability — β-lactam hydrolysis and α-pyrone volatility are both plausible — and argues for stabilised formulations or semi-synthetic analogues.

4.3. Chemical basis of activity

The cluster of diketopiperazines in F4 — cyclo(Pro-Leu), cyclo(Pro-Phe), cyclo(Pro-Val) and cyclo(Pro-Tyr), together 35.7 % of the annotated area — is mechanistically attractive. Proline-based DKPs are structural mimics of acyl-homoserine-lactone signals and can compete at LuxR/LasR-type receptors [26], and fungal metabolites of other genera interfere with Gram-negative quorum sensing in the same manner [30], which offers a straightforward explanation for the simultaneous repression of *agrA* and *lasR* and of their downstream regulons (*hla*, *icaA*, *toxA*, *algD*). In F3, terrein is a well-documented antibacterial and anti-biofilm polyketide, and in F6, 6-PP is a long-established *Trichoderma* α-pyrone antibiotic [22,23]. Because roughly a quarter of each extract escaped GC–MS annotation, these assignments should be read as hypotheses to guide fractionation rather than as proven active principles; LC-HRMS/MS, NMR and authentic standards are needed to reach MSI level 1.

4.4. Transcriptional mechanism and the anti-virulence paradigm

The pattern of repression is internally coherent for each pathogen.

In MRSA, the fall in *agrA* is matched by a fall in *hla*, consistent with Agr-dependent control of α-haemolysin, a central staphylococcal immune-evasion determinant [28], while reduced *icaA* corresponds to the 61.8 % loss of biofilm biomass. Reduced *mecA* predicts less PBP2a and sits well with the 32-fold drop in oxacillin MIC and the ΣFIC of 0.28, positioning F4 as a β-lactam-resensitising adjuvant — a route by which obsolete, low-toxicity drugs might be returned to use.

In *E. coli*, the simultaneous repression of *fimH* and *csgA* indicates an anti-adhesive, anti-curli effect, which is of particular interest for urinary-tract infection, where adhesion rather than growth rate is the limiting step. The reduction in *acrA* suggests weakened AcrAB–TolC efflux, although at 0.36-fold this needs functional confirmation by ethidium or Hoechst accumulation assays, since a decrease in transcript does not guarantee loss of pump activity.

In *P. aeruginosa*, reduced *lasR* with reduced *algD* and *toxA* is the signature of quorum-sensing quenching upstream of QS-dependent virulence and matrix production — the rationale behind quorum-sensing inhibitors as an alternative to conventional antibacterials [31] — and is relevant to the antimicrobial tolerance of P. aeruginosa biofilms [29]. Notably, *mexB* was the least affected target (0.42-fold at ½ MIC and non-significant at ¼ MIC), implying that efflux in this species is largely constitutive and LasR-independent. This serves as a useful internal negative control, showing that the extracts are not acting as generic transcriptional poisons.

Because exposures were growth-normalised and sub-inhibitory, and because validated reference genes and vehicle controls were used throughout, the common artefact of mistaking growth inhibition for specific regulation is largely avoided. Even so, mRNA abundance remains a proxy, and proteomic, enzymatic and phenotypic confirmation — haemolysis titre, PBP2a immunoblot, alginate quantification and efflux kinetics — is the necessary next step.

4.5. Selectivity and translational limits

Selectivity indices of 4.3–6.7 are encouraging for crude mixtures but fall short of what systemic use would require. Fractionation generally improves selectivity by removing cytotoxic co-metabolites, and in the case of *A. terreus* and *Penicillium* isolates the absence of mycotoxins such as citrinin and terreic acid must be demonstrated explicitly. Other limitations should be acknowledged: a single 6 h exposure point; planktonic rather than mature-biofilm exposure in the transcriptional work; batch-to-batch variability of crude extracts; the absence of in vivo pharmacokinetic data; and compound identities that remain putative.

4.6. Future directions

Work now in preparation follows six lines: bioassay-guided HPLC fractionation with LC-HRMS and NMR structure elucidation; OSMAC and co-culture approaches, with epigenetic elicitation, to activate cryptic biosynthetic clusters [6]; time-course RNA-seq to map the complete regulon and detect compensatory responses; infection models in *Galleria mellonella* followed by murine skin and pulmonary models using extract–antibiotic combinations; serial-passage experiments to test whether anti-virulence activity does in fact impose weaker selection for resistance; and cytocompatibility testing on human primary cells alongside systematic mycotoxin dereplication.

5. Conclusions

Nineteen of sixty-two fungal isolates recovered from soils of Basrah Province produced antibacterial metabolites. Three polyphasically identified strains — *Penicillium chrysogenum* F4, *Aspergillus terreus* F3 and *Trichoderma harzianum* F6 — yielded bactericidal ethyl acetate extracts (MIC 62.5–500 μg mL^{-1}; MBC/MIC = 2) whose GC–MS profiles were dominated by proline-based diketopiperazines, terrein and 6-pentyl-2H-pyran-2-one. At sub-inhibitory concentrations these extracts repressed, significantly and dose-dependently, genes governing resistance (*mecA*), efflux (*acrA*, *mexB*), adhesion and biofilm formation (*icaA*, *csgA*, *fimH*, *algD*), quorum sensing (*agrA*, *lasR*) and toxin production (*hla*, *toxA*); they reduced biofilm biomass by 55–66 % and restored oxacillin susceptibility in MRSA (ΣFIC 0.28), with selectivity indices of 4.3–6.7 on Vero cells. Fungi from these local soils are therefore credible sources of dual-action antibacterial and anti-virulence leads, although definitive attribution of activity must await purification, structural confirmation and in vivo validation.

Declarations

Ethics. No human participants or vertebrate animals were involved. The clinical bacterial isolate was a fully anonymised diagnostic specimen used with institutional approval No. Ba-2734.

Biosafety. All work followed BSL-2 practice; MRSA and potentially toxigenic fungi were handled in a Class II biological safety cabinet, and all cultures were decontaminated by autoclaving.

Data availability. Sequence data and the raw qPCR, GC–MS and dose–response datasets are available from the corresponding author on reasonable request.

Funding. This research received no external funding.

Conflicts of interest. None declared.

Acknowledgements. The author thanks the Department of Biology, College of Education for Pure Sciences, University of Basrah, for laboratory facilities, and the bacteriology laboratory of Al-Basrah Teaching Hospital for providing the clinical isolate.

References

1. Murray CJL, Ikuta KS, Sharara F, et al. Global burden of bacterial antimicrobial resistance in 2019: a systematic analysis. Lancet. 2022;399(10325):629–655.
2. World Health Organization. Bacterial Priority Pathogens List, 2024. Geneva: WHO; 2024.
3. Newman DJ, Cragg GM. Natural products as sources of new drugs over the nearly four decades from 01/1981 to 09/2019. J Nat Prod. 2020;83(3):770–803.
4. Bérdy J. Bioactive microbial metabolites. J Antibiot. 2005;58(1):1–26.
5. Kingston DGI. Modern natural products drug discovery and its relevance to biodiversity conservation. J Nat Prod. 2011;74(3):496–511.
6. Bode HB, Bethe B, Höfs R, Zeeck A. Big effects from small changes: possible ways to explore nature's chemical diversity. ChemBioChem. 2002;3(7):619–627.
7. Schoch CL, Seifert KA, Huhndorf S, et al. Nuclear ribosomal internal transcribed spacer (ITS) region as a universal DNA barcode marker for Fungi. Proc Natl Acad Sci USA. 2012;109(16):6241–6246.

8. White TJ, Bruns T, Lee S, Taylor J. Amplification and direct sequencing of fungal ribosomal RNA genes for phylogenetics. In: PCR Protocols: A Guide to Methods and Applications. Academic Press; 1990:315–322.

9. Samson RA, Visagie CM, Houbraken J, et al. Phylogeny, identification and nomenclature of the genus *Aspergillus*. Stud Mycol. 2014;78:141–173.

10. Visagie CM, Houbraken J, Frisvad JC, et al. Identification and nomenclature of the genus *Penicillium*. Stud Mycol. 2014;78:343–371.

11. Cai F, Druzhinina IS. In honor of John Bissett: authoritative guidelines on molecular identification of *Trichoderma*. Fungal Divers. 2021;107:1–69.

12. Tamura K, Stecher G, Kumar S. MEGA11: Molecular Evolutionary Genetics Analysis version 11. Mol Biol Evol. 2021;38(7):3022–3027.

13. CLSI. Methods for Dilution Antimicrobial Susceptibility Tests for Bacteria That Grow Aerobically (M07), 11th ed. Wayne, PA: CLSI; 2018.

14. CLSI. Performance Standards for Antimicrobial Susceptibility Testing (M100), 34th ed. Wayne, PA: CLSI; 2024.

15. Balouiri M, Sadiki M, Ibnsouda SK. Methods for in vitro evaluating antimicrobial activity: a review. J Pharm Anal. 2016;6(2):71–79.

16. Odds FC. Synergy, antagonism, and what the chequerboard puts between them. J Antimicrob Chemother. 2003;52(1):1.

17. Stepanović S, Vuković D, Dakić I, et al. A modified microtiter-plate test for quantification of staphylococcal biofilm formation. J Microbiol Methods. 2000;40(2):175–179.

18. Mosmann T. Rapid colorimetric assay for cellular growth and survival: application to proliferation and cytotoxicity assays. J Immunol Methods. 1983;65(1–2):55–63.

19. Livak KJ, Schmittgen TD. Analysis of relative gene expression data using real-time quantitative PCR and the $2^{-\Delta\Delta CT}$ method. Methods. 2001;25(4):402–408.

20. Bustin SA, Benes V, Garson JA, et al. The MIQE guidelines: minimum information for publication of quantitative real-time PCR experiments. Clin Chem. 2009;55(4):611–622.

21. Adams RP. Identification of Essential Oil Components by Gas Chromatography/Mass Spectrometry, 4th ed. Allured; 2007.

22. Dennis C, Webster J. Antagonistic properties of species-groups of *Trichoderma* II. Production of volatile antibiotics. Trans Br Mycol Soc. 1971;57(1):41–48.

23. Claydon N, Allan M, Hanson JR, Avent AG. Antifungal activity of the alkyl pyrone 6-pentyl-α-pyrone from *Trichoderma harzianum*. Trans Br Mycol Soc. 1987;88(4):503–513.

24. Frisvad JC, Samson RA. Polyphasic taxonomy of *Penicillium* subgenus *Penicillium*. Stud Mycol. 2004;49:1–173.

25. Nielsen KF, Månsson M, Rank C, Frisvad JC, Larsen TO. Dereplication of microbial natural products by LC-DAD-TOFMS. J Nat Prod. 2011;74(11):2338–2348.

26. Rutherford ST, Bassler BL. Bacterial quorum sensing: its role in virulence and possibilities for its control. Cold Spring Harb Perspect Med. 2012;2(11):a012427.

27. Blair JMA, Webber MA, Baylay AJ, Ogbolu DO, Piddock LJV. Molecular mechanisms of antibiotic resistance. Nat Rev Microbiol. 2015;13(1):42–51.

28. Foster TJ. Immune evasion by staphylococci. Nat Rev Microbiol. 2005;3(12):948–958.

29. Ciofu O, Tolker-Nielsen T. Tolerance and resistance of *Pseudomonas aeruginosa* biofilms to antimicrobial agents. Front Microbiol. 2019;10:913.

30. Beenker WAG, Hoeksma J, den Hertog J. Gregatins, a group of related fungal secondary metabolites, inhibit aspects of quorum sensing in Gram-negative bacteria. *Front Microbiol.* 2022;13:934235.

31. Hetta HF, Ramadan YN, Rashed ZI, et al. Quorum sensing inhibitors: an alternative strategy to win the battle against multidrug-resistant (MDR) bacteria. *Molecules.* 2024;29(15):3466.